*Journal of Applied Electrochemistry* **31**: 257–266, 2001.

# Adsorption and electrosorption at high-area carbon-felt electrodes for waste-water purification: Systems evaluation with inorganic, S-containing anions

E. AYRANCI[1] and B.E. CONWAY[2]*
[1]*Chemistry Department, Akdeniz University, PO Box 510, Antalya, Turkey*
[2]*Chemistry Department, University of Ottawa, 10 Marie Curie Street, Ottawa, ON, K1N 6N5, Canada*
*(*author for correspondence)*

Received 12 May 2000; accepted in revised form 3 October 2000

*Key words:* carbon felt, electrosorption, impurity adsorption, waste-waters

## Abstract

Removal or modification of pollutants in industrial or mineral-processing wastewaters by electrosorption at high specific-area carbon materials (felts or powders) has been envisaged in previous work. Electrodes based on high-area substrates behave as quasi-three-dimensional interfaces, thus minimizing diffusion limitation in removal of trace impurities in waters. In the present paper, processes of open-circuit adsorption and electrosorption at electrochemically polarized, high-area C-felt electrode modules are quantitatively examined by means of *in situ* electrical resistance and optical absorbance measurements made in appropriately designed cells. The effectiveness of the procedures is examined by application to the adsorption and electrosorption of a series of related S-containing anions and the kinetics of their adsorption at the C-felt electrodes have also been evaluated in two cases. The adsorbability of such impurity ions is related to their hydration properties in water.

## 1. Introduction

Intensive interest has arisen in recent years on development of procedures for purification of industrial process wastewaters [1–5] including those arising from mining and mineral processing. An attractive methodology, with the possibility of *in situ* applications, is the use of electrochemical or electrosorptive techniques employing high area [1–5] electrode or adsorbent materials such as carbon powders or preferably C-felts. Attractive C-materials are now available with large specific areas on the order of 2000–2500 $m^2\ g^{-1}$. Felts or woven meshes are preferable as they have good mechanical and structural integrity, more suitable than materials based on powders.

At plane electrodes, the rates of electrosorption of reagents are often limited by diffusion unless rapid mechanical mass transfer is achieved by electrode rotation or vibration. At high-area porous electrodes, diffusion limitation is minimized since the electrode structures behave as quasi-three-dimensional electrodes [2, 3] or adsorbent structures.

Electrochemical procedures offer the possibility of *in situ* destruction or modification to less noxious structures, of various pollutants by anodic oxidation, for example, of phenolic materials [6, 7] or xanthates. Procedures have been reviewed [2–4] or reported specifically in various papers [6, 7]. In the direct electrochemical procedures, accepted or donated electrons are the 'reagents' of the purification processes, generated *in situ*; in more indirect procedures [2], the interfacial electrode reaction is involved in producing, again *in situ*, some reactive species (e.g., $Cl_2$, $OCl^-$, $H_2O_2$, $S_2O_8^{2-}$, $Ag^{2+}$), that can modify the toxicity of impurities present in certain wastewaters.

The use of high area carbon materials also provides an important adsorptive function for accumulation of impurities with subsequent desorption (e.g., in a cyclic, pulsed system of adsorption and desorption [8]) into a vessel of smaller volume, where some other localized, possibly chemical, destruction process can be applied efficiently. In this sense, such a procedure would be analogous to the accumulation and stripping of metals into a Hg drop for trace metal determinations.

Much progress has been made in understanding the strong adsorption of organic molecules and of inorganic ions on activated carbon materials, known for a long time [9], as well as electrosorption of metals [10]. Polarization of such carbon surfaces in a suitable electrolyte can improve the extent of adsorption of ions. These advances lead to possibilities [8, 11] for electrochemical and/or adsorptive removal of various noxious ions from industrial wastewaters.

To study the adsorption of inorganic ions, their concentrations should be followed by a suitable, practical, fast responding and preferably nondestructive *in situ* method. In this respect, measurement of electrical resistance provides a convenient way as reported in works by Soffer and coworkers [12–14]. Optical absorbance measurements are also useful in following concentrations of ions absorbing in the u.v.–vis. region [15].

In a recent paper, Conway [16] directed attention to the role of ion solvation factors in the chemisorption behaviour of ions at electrode surfaces in a way complementary to the electronic interaction effects that lead to specificity of adsorption [16–18].

In the present paper, we examine the adsorption–desorption behaviour of a series of S-containing anions at electrode or adsorbent modules prepared from a C-felt having large specific area of 2500 $m^2\ g^{-1}$. The results obtained also served as 'proof of concept' for the techniques involved here for wastewater clean-up. Adsorption is studied both under open-circuit or controlled polarization conditions, the latter in anodic or cathodic directions.

## 2. Experimental details

### 2.1. *Materials*

Carbon felt used in the present work was obtained from Spectra Corp., coded as Spectracarb 2225, having a specific surface area of 2500 $m^2\ g^{-1}$. The felt electrode material was characterized electrochemically by means of cyclic voltammetry conducted in 0.1 M aq. $H_2SO_4$, giving the double-layer capacitance profiles shown in Figure 1. The apparent, projected surface area of this test electrode, 6.5 mg in weight, was 0.5 $cm^2$ and had a real area of 16.25 $m^2$. The corresponding (maximum) double-layer capacitance was 7.7 $\mu$F (real $cm^2)^{-1}$. The window for nonfaradaic charging was 1.10 V (Figure 1).

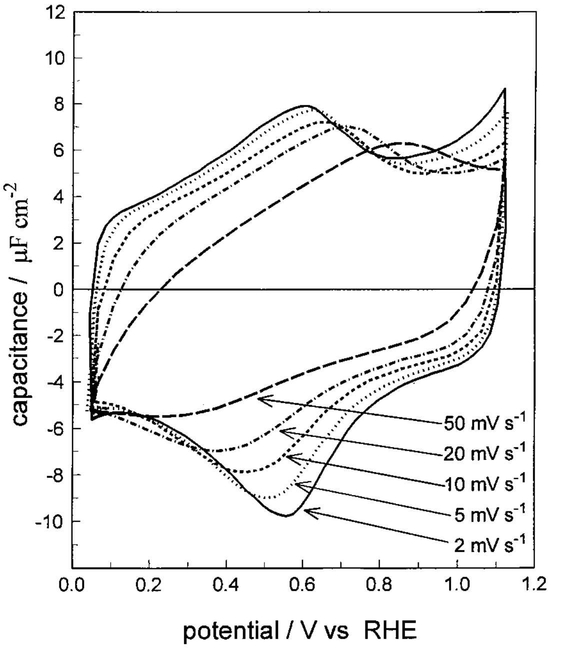

*Fig. 1.* Cyclic voltammograms, expressed as specific capacitance, obtained for Spectracarb 2225 C-felt electrode material at various indicated sweep rates in 0.5 M aq. $H_2SO_4$. (Note diminution of reversibility with increasing sweep rate due to distributed electrolyte resistance in pores.)

The inorganic salts used, sodium sulphide ($Na_2S$), sodium sulphite ($Na_2SO_3$), sodium sulphate ($Na_2SO_4$), sodium thiosulphate ($Na_2S_2O_3$), sodium dithionite ($Na_2S_2O_4$), sodium dithionate ($Na_2S_2O_6 \cdot 2\ H_2O$) and sodium thiocyanate (NaSCN) were of reagent grade. The water used in all experiments, as well as in washings and rinsings, was from a 18.2 MΩ Milli-Q UV (Millipore) water system.

### 2.2. *Treatment of the carbon-felt*

Resistance measurements were utilized to follow the adsorption of ions in part of this work. Therefore, introduction of ions from any other source into the solution is undesirable. However, some preliminary work showed that a significant quantity of ions is provided to the solution by the C-felt itself as revealed by the appreciable decreases in resistance measurements that are observed upon insertion of the C-felt into conductivity water. The origin of such ions is possibly the surface functional groups of C-felt or of any ions adventitiously introduced in the preparation of the C-felt. Various possible functional groups that might be present at C surfaces have been tabulated by Conway [19], Kinoshita [20] and Sihvonen [21]. The problem of release of undesired ions by porous carbon materials was also reported by Soffer and Folman [13].

To avoid such ions desorbing during the adsorption experiments, a C-felt sample having an approximate apparent area of 250 $cm^2$ was placed in a flow-through washing cup and washed, batchwise, with 5 L of warm (60 °C) conductivity water for two days with $N_2$ bubbling to exclude $CO_2$ and $O_2$. Outcoming water from each batch was tested conductometrically for the completeness of washing. The washed C-felt modules were then dried under vacuum at 120 °C and kept in a desiccator for further use.

The C-felt was cut in desired dimensions, weighed accurately, then formed into cylindrical modules, rolled and tied by means of a thin gold wire for introduction into the adsorption cell.

### 2.3. *Resistance measurements for open-circuit adsorption*

For open-circuit adsorption (i.e. without external polarization of the C-felt), a glass cell having two compartments that could be called the adsorption and conductivity limbs was constructed. After the whole cell, including the C-felt placed in the adsorption compartment, had first been evacuated, a known volume of the adsorbate solution was introduced under vacuum into the adsorption compartment from a burette fitted to the cell with a glass joint. After making sure that all the air in the pores of C-felt had been removed, the vacuum was released and felt/solution system was allowed to attain adsorption equilibrium. Then, by tilting the cell, the solution was transferred to the lower conductivity compartment that was equipped with a pair of previously calibrated platinized-platinum electrodes. The resistance of the solution was then monitored over a lengthy period of time by a Boonton 5110 LCR meter to which the Pt electrodes were connected. The achievement of adsorption equilibrium was indicated by approach of the resistance towards a constant value. Excellent empirical relations were observed between concentration and measured reciprocal resistance for each of the salt solutions studied and served as calibration relations for conversion of resistance readings into corresponding concentrations.

The amount of adsorbed salt per unit mass of C-felt was calculated from the following simple equation,

$$M = \frac{(c - c_0)V}{m} \qquad (1)$$

where $c_0$ and $c$ are the concentrations at the beginning and at the equilibrium adsorption state, respectively, $V$ is the volume of solution and $m$ is the mass of the C-felt module.

### 2.4. *Electrolytic cell for polarization of C-felt*

In preliminary electrochemical experiments, C-felt was used as the working electrode, a platinum gauze as the counter electrode and a silver/silver oxide electrode as the reference electrode. However, due to the huge surface area of the working-electrode compared with that of the counter electrode, passage of even a very small charging current at the C-electrode caused undesired faradaic reactions leading to visible gas evolution at the smaller counter electrode. Such reactions may also be producing or consuming ions that affect the resistance measurements. Hence, it was necessary to replace the platinum gauze counter-electrode with another C-felt electrode of about the same area as that of the working electrode.

The electrochemical cell, shown in Figure 2, was V-shaped in its upper part. One arm contained the working electrode and the reference electrode, while the other arm contained the counter electrode and a thin tube through which $N_2$ gas was passed to bubble through the solution for the purposes of mixing and eliminating any dissolved $CO_2$.

### 2.5. *Procedure for potential and resistance measurements*

The two C-electrodes which had been weighed, rolled and tied by Au wires were placed into each arm of the cell and the whole cell was evacuated to remove all air in the pores of the C-electrodes. A known volume of a 0.1 M salt solution was introduced into the cell from the burette fitted to one of the cell arms by a glass joint. Further evacuation was applied after adding the solution to remove residual air and to enable the solution to gain access to the whole C surface. The vacuum was then released, the burette removed, and the reference electrode and $N_2$ bubbling tube were inserted. Working, counter and reference electrodes were connected to a Hokuto Denko HA-301 potentiostat/galvanostat. An external Fluke 8050A digital multimeter was also connected to the potentiostat/galvanostat for digital reading of potential. In the galvanostatic mode, a constant current of about ± 10 mA was passed through the cell. Potential and resistance measurements were recorded from the respective meters every 5–10 min. After the potentials had become steady, the polarity was reversed.

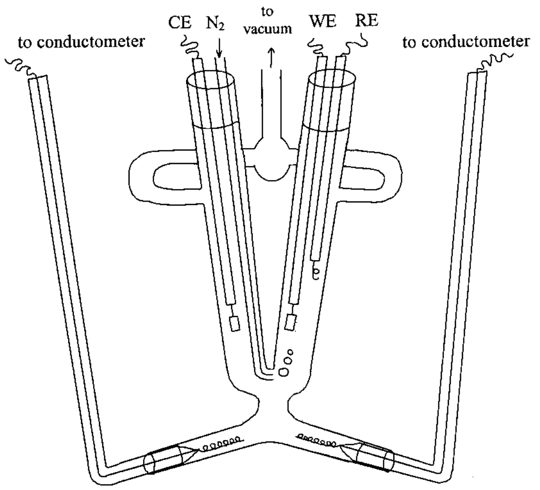

*Fig. 2.* Schematic diagram of electrolytic cell used for polarization of C-felt and *in situ* resistance measurements.

### 2.6. *Modified cell for optical absorbance measurements*

Among the salts studied, NaSCN showed a clear absorbance shoulder, flat enough to carry out reliable quantitative measurements at 215 nm. To follow its concentration during adsorption, the cell described above was modified by replacing the conductance element by a quartz spectrophotometer cell, enabling *in situ* concentration measurements to be made by means of a Cary 1E type u.v.–vis. spectrophotometer interfaced to a computer. The quartz cell element could be accommodated in the spectrometer's front sample compartment.

Following the same procedure described above for evacuation of the whole cell, introduction of solution and completion of connections of the electrodes to the potentiostat/galvanostat, a black curtain was spread over the cell to prevent any interference from external light. This time a Teflon tube, connected to the tip of the thin $N_2$ bubbling tube, was lowered all the way down in the u.v. cell to a level just above the light path to accomplish effective mixing.

Absorbance was followed as a function of time from the monitor using the software provided by the manufacturer of the spectrophotometer, employed in the kinetics mode. This design provided great flexibility in the experimental procedure. For example, when the concentration of solution dropped to low values, a small known volume of concentrated solution could be added by means of a micrometer burette before any application of potential. It was also possible to follow the kinetics of adsorption both before and after application of potential. Since absorbance, not the resistance, was now being followed, a Pt-gauze could also be used instead of C-felt as the counter electrode in this part of the work. One restriction of the method was that the concentration of the solution had to be kept low enough for Beer's law to be obeyed. At such low concentrations, due to the high resistance of the solutions, only a small polarization current could be passed ($<1$ mA). If it were possible to pass higher currents, further and faster increase in the extents of adsorption could have been observed.

## 3. Results and discussion

### 3.1. *Open-circuit adsorption*

0.1 M solutions of sodium salts of a series S-containing anions were allowed to reach adsorption equilibrium with the C-felt. The equilibrium concentrations were determined from resistance measurements using the appropriate calibration data referred to earlier. The amounts of adsorbed or, in some cases, desorbed salt ions were calculated using Equation 1. The results are presented in Table 1 where the percentage coverage, $\theta$, of the C surface is also given in the last column. $\theta$ was calculated on the basis of the total specific surface area value of 2500 $m^2\ g^{-1}$ provided by the manufacturer, and the approximate value of $10^{19}$ sites per $m^2$ of surface using the following equation,

$$\theta = \frac{(c_0 - c)VN_0}{10^{19} \times 2500m} \times 100 \tag{2}$$

where $c_0$ and $c$ are the original and equilibrium concentrations, respectively, $V$ is the volume of the solution, $N_0$ is Avogadro's number and $m$ is the mass of the C-felt electrode used. Since the surface coordination structure of the C fibrils is unknown, the figure of $10^{19}$ sites $m^{-2}$ is an order-of-magnitude figure based on the covalent radius of the C atom of 0.077 nm and a (100)-type c.p. square lattice. At a (111)-type surface lattice, the figure would be 23% greater.

*Table 1.* Equilibrium concentration, extent of adsorption and percentage coverage values for a series of Na salts of S-containing anions adsorbed at the C-felt modules

| Salt | Equilibrium concentration /mol $L^{-1}$ | $10^5 \times$ amount of adsorption /mol (g C-felt)$^{-1}$ | Coverage, $\theta$ /% |
|---|---|---|---|
| $Na_2S$ | 0.0699 ± 0.0035 | 37.1 ± 1.86 | 0.89 ± 0.05 |
| $Na_2SO_3$ | 0.0948 ± 0.0047 | 6.9 ± 0.35 | 0.28 ± 0.01(4) |
| $Na_2SO_4$ | 0.1039 ± 0.0052 | −4.4 ± 0.22 | – |
| $Na_2S_2O_3$ | 0.0972 ± 0.0049 | 3.4 ± 0.17 | 0.08 ± 0.04 |
| $Na_2S_2O_4$ | 0.0972 ± 0.0049 | 3.7 ± 0.19 | 0.09 ± 0.04(5) |
| $Na_2S_2O_6$ | 0.1031 ± 0.0052 | −3.6 ± 0.18 | – |
| NaSCN | 0.0844 ± 0.0042 | 20.2 ± 1.01 | 0.49 ± 0.02(5) |

Since $Na^+$ constitutes the cation of all the salts studied, the variations in the extents of adsorption reflect mainly the specificity of adsorption of the anions. $S^{2-}$ exhibits the strongest adsorption. Next, in order, comes the $SCN^-$ ion, while, relatively, $SO_4^{2-}$ shows some small apparent rejection from the surface possibly due to preferred water adsorption and to the strongly hydrated state of the $SO_4^{2-}$ ion, cf. [16]. The results for these three ions are not surprising when the hierarchy of shifts of potential of zero charge of Hg by adsorption of various ions given by Conway [16] are examined. Among the ions studied here, only the above three were included in Conway's list and they show the same order of specific adsorption tendency. Conway [16] also showed that $S^{2-}$ exhibits the strongest adsorption among the 15 ions he compared. $SO_4^{2-}$ had very close to zero specific adsorption level.

The hydration behaviour of various S– and Cl–oxyanions has been studied extensively by the present authors [22, 23] through partial molar volume and compressibility measurements. It was found that size, shape and charge effects play an important role in determining the hydration behaviour of these ions. Based on the results presented in Table 1, these factors are evidently also effective in determining the adsorption behaviour of the S-containing ions. Actually, the adsorption behaviour is expected to be closely related to the hydration behaviour. Thus, it is quite probable that each of these salts is being adsorbed from the S-centre of the S-containing anions, except $SO_4^{2-}$ where the S is protected by four O ligands. As a free monatomic doubly-charged ion, $S^{2-}$ exhibits the strongest adsorption, as at Hg. The presence of other atoms ligated to S in other anions, as well as charge reduction in the case of $SCN^-$, causes diminution in the relative extents of adsorption. The $SCN^-$ ion, having a single negative charge, has almost half the adsorption value of $S^{2-}$. In the case of S-oxyanions, the distribution of O ligands around the S atom(s) determines the extents of their adsorption on the C surface. Electronic contact of S atoms with the C surface is prevented by the O atoms in $SO_4^{2-}$ and $S_2O_6^{2-}$. Therefore, a slight negative adsorption (i.e., a slight repulsion of these ions by the C surface) was observed, probably due to the strong hydration of these doubly-charged anions, the adsorption of which would have to displace previously adsorbed $H_2O$ molecules.

Because of the huge specific surface area of the C-electrodes, the percentage coverage values, $\theta$, given in Table 1, are actually relatively low. They are less than one percent, even for the most strongly adsorbing $Na_2S$. This is probably because a fraction of the adsorption sites are in very small pores which may not be accessible to the ions. It was believed that the amount of adsorption, and thus the percentage coverage, could be substantially increased by charging the electrodes.

### 3.2. *Influence of polarization on adsorption*

The purpose of using C-felt as both the working and counter electrodes was to increase the surface area of the counter electrode and thus prevent gas evolution coupled with ion-producing (or consuming) faradaic reactions. However, an experiment with $Na_2SO_3$ carried out in a cell whose half-cells were separated by a glass frit showed that this purpose was not completely achieved because the pH in the two half-cells then became considerably changed, depending on the sign of polarization. Similar pH changes were also observed with $Na_2SO_4$ and NaSCN upon polarization of the electrodes. Such large pH changes were not observed in experiments with the same salt in a cell where there was no separation of the two half-cells. This showed that at least $H^+$ and $OH^-$ ions, produced at the two electrodes, become neutralized in the unseparated cell. Thus, at the electrodes, apart from the adsorption of the salt ions, the following interfacial reactions

$$C + H_2O + e^- \rightarrow C\text{–}H + OH^- \qquad (3)$$

$$C + H_2O \rightarrow C\text{–}O + 2\,H^+ + 2\,e^- \qquad (4)$$

$$C + H_2O \rightarrow C\text{–}OH + H^+ + e^- \qquad (5)$$

are possibly occurring at the high-area, active C surfaces, as suggested by Soffer and Folman [13], but fortunately at least some of the ions become neutralized within a combined cell. The resistance of the solution will be affected by two opposing factors. The produced ions that are not neutralized cause a decrease, while a net adsorption of ions causes an increase in the resistance of the solution. It would hence be meaningless to convert the measured resistances into concentrations using calibration data that were obtained for pure salt solutions. However, it is believed that the resistance values alone may still reflect the trends in adsorption of the salts.

The resistance against potential curves are given in Figures 3 and 4 for $Na_2SO_4$ and $Na_2SO_3$, respectively. Both salts exhibit similar trends in variation of resistance with changes of potential. On the basis of the above discussion, it is believed that data in both figures reflect mainly the adsorption behaviour of both ions of the salts under study. During the initial positive polarization of the working electrode, the resistance of the solutions, and thus net adsorption of ions, is increasing. Here, the negative $SO_4^{2-}$ or $SO_3^{2-}$ ions are probably being adsorbed on the working electrode as it is positively charged and $Na^+$ ions are being adsorbed at the counter electrode. Although these ions are adsorbed at the surface (i.e., with respective surface excesses), they attract more oppositely charged ions than those of like charge in the double layer. Therefore, there will be a net depletion of ions which thus increases the resistance of the solutions, as observed.

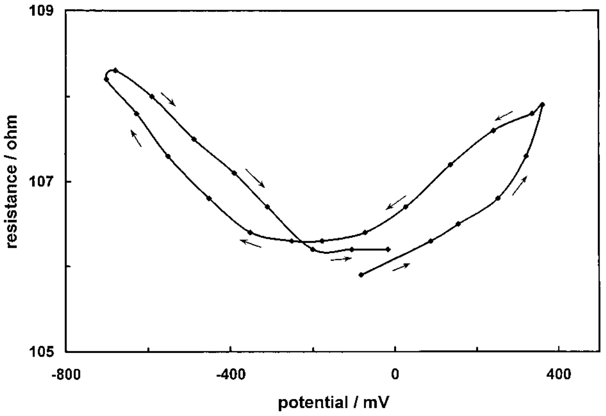

*Fig. 3.* Adsorption of $Na_2SO_4$ from 0.1 M solution on C-felt as reflected by the resistance of solution as a function of potential against an Ag/AgO reference electrode. Arrows show directions of polarization.

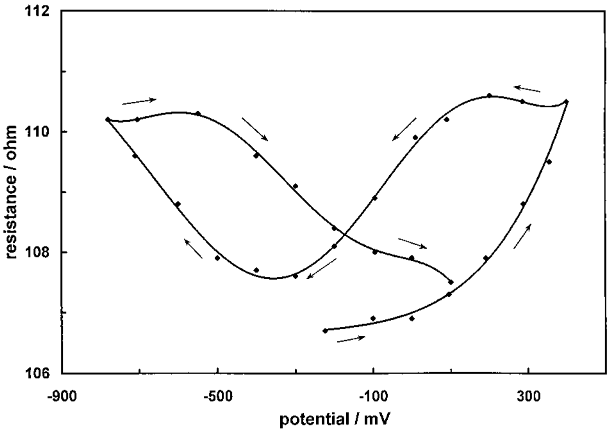

*Fig. 4.* Adsorption of $Na_2SO_3$ from 0.1 M solution on C-felt as reflected by the resistance of solution as a function of potential against an Ag/AgO reference electrode. Arrows show directions of polarization.

When the polarity of the electrodes is reversed, at first some of the ions adsorbed as a result of the initially opposite polarization are desorbed, causing a net initial decrease in resistance of the solutions. As the negative charging of the working electrode is continued, then $Na^+$ ions start to become adsorbed at the working electrode, while $SO_4^{2-}$ or $SO_3^{2-}$ ions begin to become adsorbed at the counter-electrode. This causes again an increase in resistance of the solutions. At the negative end of the potential scan, when the polarity of the electrodes is reversed, again a decrease in resistance due to desorption of ions adsorbed under the effect of opposite polarization is observed. If the positive charging were continued, net adsorption of oppositely charged ions would result, causing an increase in resistance again, as was observed in the other direction of polarization. It is to be noted that throughout the whole potential range, values of resistance change for desorption are greater than those for adsorption. This is believed to be an example of the well-known hysteresis effect that is frequently observed in adsorption/desorption and also

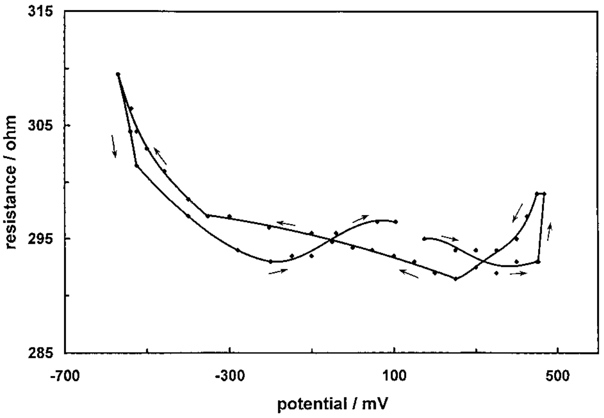

*Fig. 5.* Adsorption of NaSCN from 0.1 M solution on C-felt as reflected by the resistance of solution as a function of potential against an Ag/AgO reference electrode. Arrows show directions of polarization.

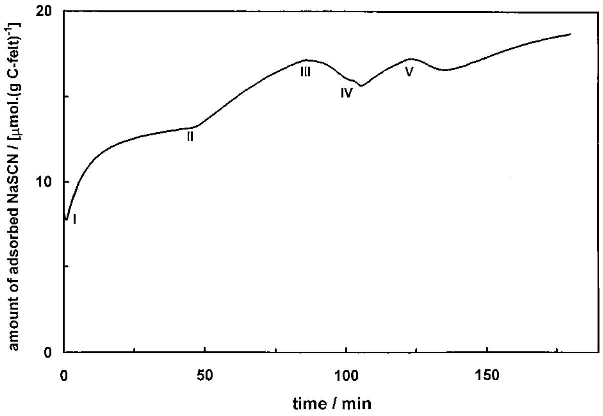

*Fig. 6.* Adsorption of NaSCN as a function of time during a series of polarization operations. Both working and counter electrodes are C-felt.

in magnetization/demagnetization and solid state transitions. Everett and coworkers, in a series of papers [24–26], have treated this phenomenon in detail, including examples of hysteresis in adsorption phenomena.

Slightly different behaviour was observed for NaSCN whose resistance against potential diagram is presented in Figure 5. There is a crossover of the plots on the positive potential side. On the negative potential side, there seems to be a kind of reverse hysteresis. It is difficult to explain this behaviour. Probably, in this case, the produced ions, rather than the adsorbing ions, are playing the major role in determining the resistance changes. Fortunately, NaSCN absorbs electromagnetic radiation in the u.v. region, so that its adsorption could also be studied by following absorbance changes instead of resistance. The results of such a study are given in the following section in detail and provide further support for the processes occurring at the C-electrodes, proposed above for $Na_2SO_4$ and $Na_2SO_3$.

### 3.3. *Adsorption on open-circuit and upon polarization as monitored by absorbance measurements*

Although, it could only be applied to NaSCN among the salts studied, absorbance measurements provided convincing evidence about what is actually taking place at the C-electrodes. Adsorption of $SCN^-$ ions was followed by recording absorbance as a function of time during adsorption on open-circuit, followed by polarization of the electrodes. The recorded absorbance data were later converted into concentration changes using previously obtained calibration curves. Finally, the amount of adsorbed NaSCN per unit mass of C-felt was calculated from Equation 1 using $c$ as the concentration at any time instead of the equilibrium concentration. A series of three experiments were performed.

In the first experiment, adsorption of $SCN^-$ was followed with time using C-felt for both working and counter-electrodes during the following successive operations: (I) Open-circuit adsorption, (II) negative polarization of the working electrode by passing −0.4 mA current galvanostatically, (III), (IV) and (V) reversing the polarity of electrodes alternately by passing +0.4 or −0.4 mA currents, galvanostatically. The results are shown in Figure 6 where the starting point of each operation is marked with the corresponding Roman numeral. During the open-circuit adsorption (I), a clear exponential decay of concentration and thus an increase in adsorption is observed.

Data in this region were analysed on the basis of first-order kinetics and a rate-constant of 0.060 $min^{-1}$ was derived. Kinetic analysis will further be dealt with below in relation to the third type of experiment in this series. When the extent of adsorption had reached a plateau, negative polarization of the working electrode (II) caused an increase in rate of adsorption. It should be recalled that the counter electrode is being positively charged during this operation. When the increase in adsorption started just to slow down, reversing the polarity (III) caused a decrease in adsorption, or more correctly a desorption. Reversing the polarity for the second time (IV), increased the adsorption after a short period of continuation of desorption. Interestingly enough, when the polarity of the electrodes was reversed for the last time (V) and charging was continued for a relatively longer period, it was observed that a desorption followed by an adsorption took place after passing through a minimum.

In a second experiment, the same system was used but the order of polarization steps was changed. That is, after the open-circuit adsorption, the working electrode was polarized first with positive charge and then with charges alternately changing in sign. The results are not shown here since the adsorption against time graphs for this experiment showed exactly the same trend as that seen in Figure 6. That is, an initial increase in adsorption on open circuit, an increase in rate of adsorption during positive polarization of the working electrode and then a desorption following reversal of polarity of the electrodes. A region of initial desorption followed by an adsorption was also observed during a longer period of negative polarization of the working electrode.

For systems of the type treated in the present paper, involving differential adsorption of cations and anions at a working and a counter electrode, the behaviour resulting from polarization has been discussed by Oren and Soffer [27, 28]. Based on their type of analysis, four complementary mechanisms can be suggested as being responsible for the above processes occurring at the electrodes. Diagrammatic representation of the processes of adsorption at the electrodes during the successive operations of the above experiments, is shown in Figure 7, and helps to explain these mechanisms. (A) It is believed that during the initial open-circuit adsorption process, mainly $SCN^-$ ions (shown by $X^-$ in Figure 7) are being adsorbed. If $Na^+$ ions were also being adsorbed, negative adsorption would not be observed for any of the salts given in Table 1.

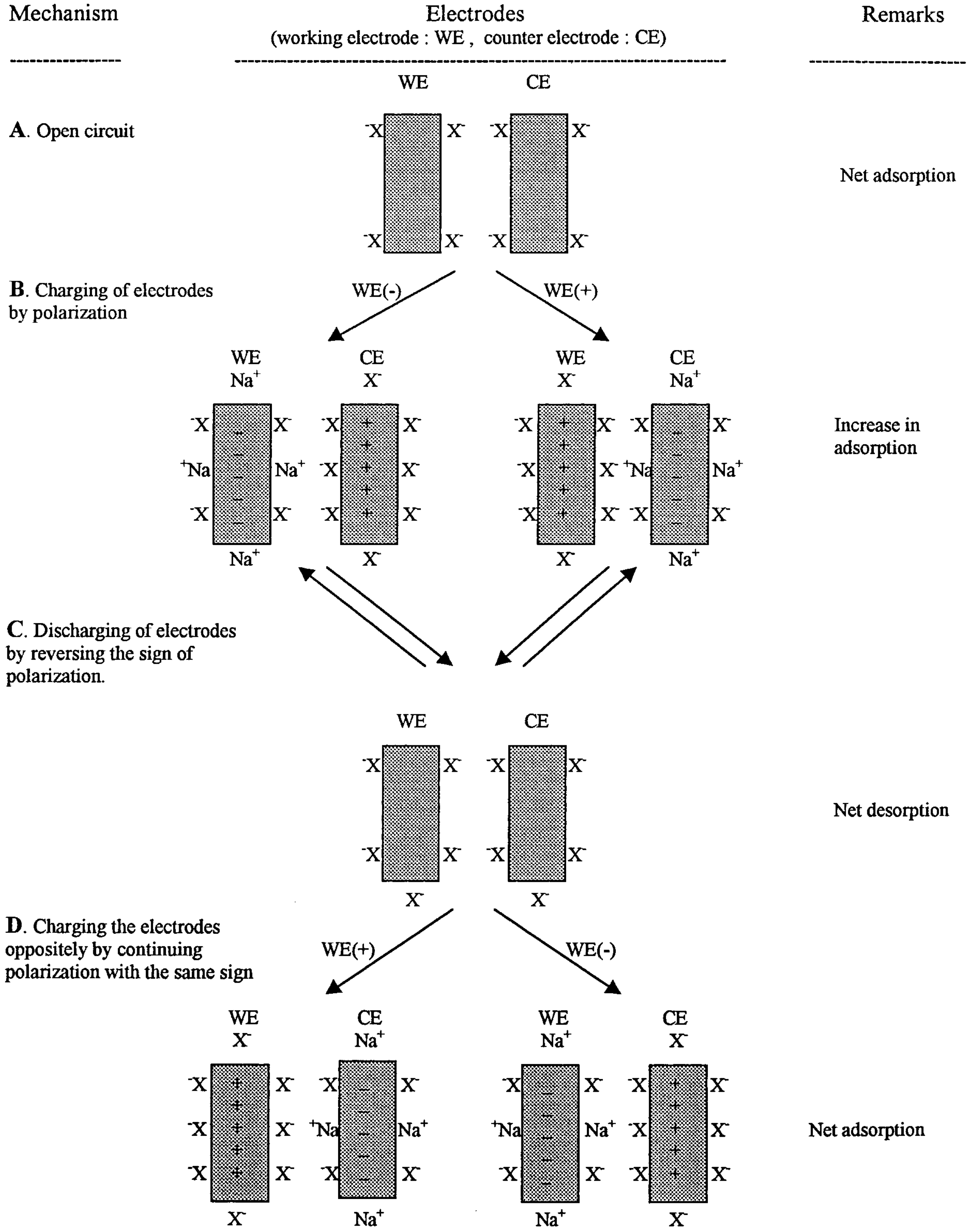

*Fig. 7.* Schematic representation of mechanism of adsorption of anions $X^-$ during various stages of the adsorption process.

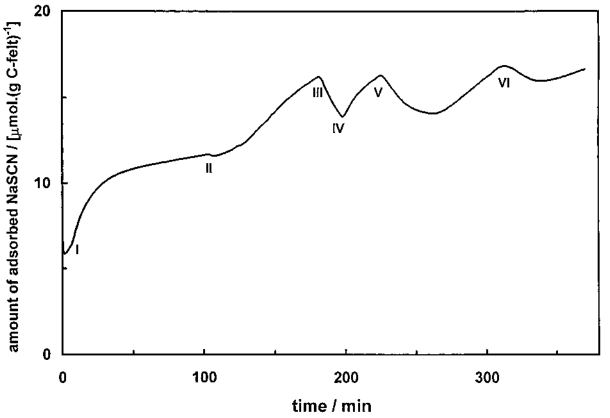

*Fig. 8.* Adsorption of NaSCN as a function of time during a series of polarization operations. Working electrode is C-felt and the counter electrode is Pt-gauze.

$Na^+$ ions become adsorbed only under the influence of externally applied electrostatic attraction forces. (B) On the one hand, when the working electrode is charged negatively and thus the counter electrode positively, the working electrode attracts and adsorbs $Na^+$ ions while the counter electrode adsorbs more $SCN^-$ ions, causing an overall increase in adsorption. On the other hand, if the working electrode is charged positively and thus the counter electrode negatively, the two electrodes change roles, but eventually the same overall increase in adsorption results.

The overall charging behaviour of the C-felt electrode material used in the present work (relevant to the above mechanism) is illustrated in the double-layer capacitance profiles shown in Figure 1; these were generated by cyclic voltammetry (see Section 2.1) conducted at the various sweep rates indicated in the figure. The overall potential-dependence of capacitance provides primary characterization of the electrochemical properties of the C-felt electrode material and determines the time scales of changes of potential (see Figures 7, 8 later) upon polarization at constant currents.

The $SCN^-$ ions, specifically adsorbed on open-circuit, are believed to remain adsorbed during the polarization operations, starting with mechanism (B) of Figure 7. (C) Whether the electrode surfaces were already positively or negatively charged, when the polarity of the two electrodes is reversed, they first release at least some of the ions adsorbed on them during the previous opposite polarization period. This desorption continues until discharging is complete. It should be recognized that the extent of desorption associated with this mechanism is less than that of adsorption associated with mechanism (B). This is due to the fact that some of the adsorption sites, especially those in small pores that were difficult to be accessed on open-circuit, become accessible on account of the externally applied polarization force. Especially some of the $SCN^-$ ions adsorbed in such pores prefer to remain adsorbed as they do in the case of adsorption at open-circuit. It should also be noted that reversing the polarization at any instant during discharging of the electrodes returns the situation back to that of the mechanism described in (B) and (D). After the electrodes have been discharged, if the same polarization is continued, they start to attract oppositely charged ions since they themselves start to gain charges opposite to what they had before. This causes an increase in adsorption again.

The above mechanism explains the trend observed in Figure 6. A small detail in this figure may, however, need further explanation. At the start of operation IV, a small amount of desorption is observed for a short period of time before the expected re-adsorption starts. This is possibly because the polarity of the electrodes was reversed after the turnover associated with mechanism (D) above had just started. When the polarity was changed, the electrodes release those ions that had just started to adsorb first and then begin to attract oppositely charged ions.

Finally, in the third type of experiment, the same system was studied by replacing the C-felt counter-electrode with Pt gauze. The purpose of this experiment was to explore the processes taking place in a single adsorbing C-electrode, as the surface of Pt gauze is negligibly small compared to that of the C-felt working electrode. The possible undesired faradaic reactions producing some ions do not then obscure the adsorption trend to be observed in this case, since absorbance rather than resistance is being measured. The results of this experiment are shown in Figure 8 where the polarization operations are again marked by Roman numerals. In this case, only the working-electrode need be considered in the interpretation of the adsorption behaviour because the Pt-gauze counter electrode adsorbs negligibly compared to the working electrode.

The initial open-circuit adsorption (I) was again analysed kinetically by assuming it is of first order. A rate constant of 0.052 $min^{-1}$ was obtained. The rate constant value, already reported above for the first of this series of experiments, is in fair agreement with this value. However, it is believed that the latter is more reliable, because the open-circuit adsorption was continued for a longer period of time and thus a better fit could be obtained. In Figure 9, both the fitted line and experimental data points in 6 min intervals for the first 40 min of adsorption are presented as natural logarithm of ratio of the initial absorbance to the absorbance at any time against time to show the goodness of fit. It will be recalled that only $SCN^-$ ions are being adsorbed at the surface on open-circuit. The adsorption and the rate equations can be represented in the following forms, involving displacement of previously adsorbed $H_2O$ molecules:

$$\mathrm{C{-}H_2O + SCN^- \rightarrow C{-}SCN^- + H_2O} \tag{6}$$

$$v = k[\mathrm{SCN^-}] \tag{7}$$

where $v$ is the rate and $k$ is the rate-constant. It should be recognized that this is a pseudo-first order process, as the

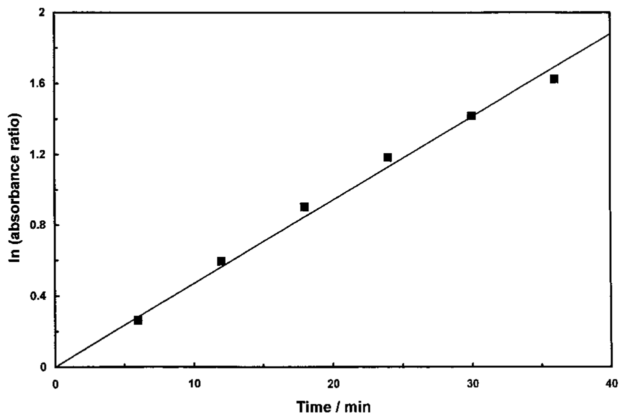

*Fig. 9.* Natural logarithm ratio of the initial absorbance to the absorbance at any time during open-circuit adsorption of NaSCN. Key: (——) line fitted according to the first order kinetics, (■) experimental data points.

concentration of water or number of available adsorption sites is essentially constant for dilute solutions.

In operation (II) of Figure 8, the C-electrode was positively charged by passing a current of +0.35 mA galvanostatically. Application of potential causes an increase in the rate of adsorption. The C-electrode was then discharged at (III) and this operation caused the desorption of some of the $SCN^-$ ions adsorbed in (II). The sign of polarization was reversed at (IV), possibly while the discharging was not yet complete so that sudden re-adsorption starts. The situation is analogous to switching from mechanism (C) to (B) of Figure 7 at this point. At (V), negative polarization of the C-electrode is applied and causes an initial desorption due to discharging, followed by adsorption of $Na^+$ ions after a minimum in the adsorption curve in Figure 8, due to the continuing negative polarization. Finally, reversal of the polarity for a relatively long period starting at (VI) causes an initial desorption of $Na^+$ ions, together with the $SCN^-$ ions in the double-layer, due to discharging. This becomes followed by adsorption of $SCN^-$ ions due to positive charging of the discharged working electrode. The difference in adsorption values at the two minima, following the operations (V) and (VI), should be related to the number of sites made accessible for $SCN^-$ ions due to polarization of the electrode.

### 3.4. *Comment on the removal of NaSCN and regeneration of the surface of the C-felt*

The extent of removal of $SCN^-$ ions from the solution by adsorption depends, of course, on the concentration of the solution, its volume, the mass of C-felt and the amount of charge loaded on the C-felt when an external potential is applied. A typical set of values for the first three of the above four parameters, and the resulting relative decrease in concentration, is provided here just to give an idea about how effective is the anion removal process. For example, in the first of the series of three experiments mentioned above, the initial NaSCN concentration was $5 \times 10^{-4}$ M, the volume of solution was 20 mL and the total mass of the C-felt electrode was 0.4965 g. The amount of charge loaded during each operation can be calculated from the current passed and the time, and the corresponding potential changes are determined by the capacitance behaviour (Figure 1). Since several alternating polarization operations have been applied to elucidate the adsorption mechanism, the amount of charge supplied just to remove the ions cannot be given here. In this particular experiment, the concentration was lowered to $1.6 \times 10^{-4}$ M on open-circuit adsorption. This corresponds to 68% reduction in the ion's concentration. After several polarization operations, it was further lowered to $2.4 \times 10^{-5}$ M corresponding to a 95% reduction in concentration. It should be noted that, even at such a high level of removal, the percentage coverage of the C-felt electrode is as low as 0.05%, indicating opportunities for application of the procedures to solutions of substantially higher 'pollutant' salt concentrations.

Of course, ultimately, the uptake of such species is limited by the fact that not all the BET area available to gas adsorption is accessible to solution species owing to the presence of very fine pores in the pore distribution. Other factors involved in limiting the performance of the felt materials for pollutant removal are that rates of adsorption and desorption are slow (Figures 4, 7 and 8), as are rates of regeneration owing to slow diffusion within the porous matrix. To regenerate the surface of the C-felt, the ions must be desorbed. It was found that partial desorption can be achieved by discharging the electrodes. A further treatment is required for a more complete regeneration. This may involve flushing by hot water, as desorption is expected to increase with temperature, but is otherwise slow or hysteresis effects [26] are involved (e.g. as in Figures 3 and 4).

## 4. Conclusions

Procedures based on adsorption and electrosorption of trace salt ions at high area C-felt electrode modules are shown to be effective for removal of such ions from dilute aqueous solutions of a series of S-containing anions serving as model systems for wastewater purification. The adsorptive effectivenesses are related to the factors such as charge, size and shape of ions that play important roles in their hydration behaviour.

*In situ* solution–resistance measurements were found to provide information about the general trend in adsorption (e.g., of $Na_2SO_4$ and $Na_2SO_3$). However, more convincing and accurate quantitative information was obtained from *in situ* optical absorbance measurements for $SCN^-$ which absorbs in the u.v. region. The monitoring of the changes in absorbance of solution was proven to be a useful technique for the adsorption studies providing not only quantitative adsorption data but also kinetic information.

Polarization of C-felt surfaces caused increases in rate of adsorption of ions. It was also found that reversing the polarization for sufficiently long periods of time caused an initial desorption of ions due to discharging of the electrode, followed by re-adsorption of oppositely charged ions. A proposed mechanism helps to explain the adsorption of behaviour of ions on open-circuit and upon polarization.

High area C-felt materials were found to be specially effective in removal of noxious ions such as $SCN^-$, $S^{2-}$ etc. chosen as models for polluting ions in wastewaters.

## Acknowledgements

Grateful acknowledgement is made to the Natural Sciences and Engineering Research Council of Canada for support of this work on a Strategic Grant. One of us (E.A.) acknowledges a sabbatical leave from the Akdeniz University, Turkey, and the authors thank Dr W. G. Pell for Figure 1, arising from other work in this laboratory.

## References

1. B. Fleet and S. Das-Gupta, *Nature* **263** (1976) 122.
2. T.L. Rose, O. Murphy, E. Rudd and B.E. Conway (Eds), 'Water Purification by Photocatalytic, Photoelectrochemical and Electrochemical Processes', Conference Proceedings, Vol. **94-19**, The Electrochemical Society, Pennington, NJ (1994).
3. D. Pletcher and N. Weinberg, *Chem. Eng.* **99**(8) (1992) 98.
4. D. Pletcher and N. Weinberg, *Chem. Eng.* **99**(11) (1992) 132.
5. B. Fleet, *Coll. Czech. Chem. Comm.* **53** (1988) 1007.
6. M. Gatrell and B. MacDougall, *J. Electrochem. Soc.* **146** (1999) 3335.
7. A. Boscolo Boscoletto, F. Gottardi, L. Milan, P. Pannocchia, V. Tartari, M. Tavan, R. Amadelli, A. De Battisti, A. Barbieri, D. Patracchini and G. Battaglin, *J. Appl. Electrochem.* **24** (1994) 1052.
8. T. Otowa, T. Tomita, H. Oda and M.D. Andelman, *in* F. Meunier (Ed), 'Fundamentals of adsorption' (Elsevier, Amsterdam, 1998), p. 945.
9. J.J. Kipling, 'Adsorption from Solutions of Non-electrolytes' (Academic Press, London, 1965).
10. D.M. Kolb, *in* C.W. Tobias and H. Gericher (Eds), 'Adv. Electrochem. Electrochem. Eng.', (Wiley, New York) **11** (1978) 125.
11. B. MacDougall, M. Gattrell, S. Tajwar, D. Fulton and C.J. Hemming, *in* T.L. Rose, O. Murphy, E. Rudd and B.E. Conway (Eds), 'Water Purification by Photocatalytic, Photoelectrochemical and Electrochemical Processes', Conference Proceedings, Vol. **94-19**, The Electrochemical Society, Pennington, NJ (1994), p. 99.
12. J. Koresh and A. Soffer, *J. Electrochem. Soc.* **124** (1977) 1379.
13. A. Soffer and M. Folman, *J. Electroanal. Chem.* **38** (1972) 25.
14. Y. Oren, H. Tobias and A. Soffer, *J. Electroanal. Chem.* **162** (1984) 87.
15. B.E. Conway, R.G. Barradas and T. Zawidzki, *J. Phys. Chem.* **62** (1958) 676.
16. B.E. Conway, *Electrochim. Acta* **40** (1995) 1501.
17. R. Parsons, *J. Electroanal. Chem.* **5** (1963) 397.
18. D.C. Grahame, *Chem. Rev.* **47** (1947) 441.
19. B.E. Conway, 'Electrochemical Supercapacitors' (Kluwer Academic/Plenum, New York, 1999).
20. S. Kinoshita, 'Carbon' (Wiley, New York, 1988).
21. V. Sihvonen, *Trans. Faraday Soc.* **34** (1938) 1062.
22. B.E. Conway and E. Ayranci, *J. Chem Soc. Faraday Trans. I* **79** (1983) 1357.
23. B.E. Conway and E. Ayranci, *J. Solution Chem.* **28** (1999) 163.
24. D.H. Everett and W.I. Whitton, *Trans. Faraday Soc.* **48** (1952) 749.
25. D.H. Everett and F.W. Smith, *Trans. Faraday Soc.* **50** (1954) 187.
26. D.H. Everett, *Trans. Faraday Soc.* **51** (1955) 1551.
27. Y. Oren and A. Soffer, *J. Appl. Electrochem.* **13** (1983) 473 and 479.
28. Y. Oren and A. Soffer, *J. Electrochem. Soc.* **125** (1978) 869.